Optical Coherence Tomography Angiography of Optic Disc Perfusion in Glaucoma

Yali Jia, PhD[1], **Eric Wei, BS**[1], **Xiaogang Wang, MD**[1], **Xinbo Zhang, PhD**[1], **John C. Morrison, MD**[1], **Mansi Parikh, MD**[1], **Lori H. Lombardi, MD**[1], **Devin M. Gattey, MD**[1], **Rebecca L. Armour, MD**[1], **Beth Edmunds, MD**[1], **Martin F. Kraus, MS**[2,3], **James G. Fujimoto, PhD**[3], and **David Huang, MD, PhD**[1]

[1]Casey Eye Institute, Oregon Health and Science University, Portland, OR 97239, USA

[2]Pattern Recognition Lab and School of Advanced Optical Technologies (SAOT), University Erlangen-Nuremberg, D-91058 Erlangen, Germany

[3]Department of Electrical Engineering and Computer Science, and Research Laboratory of Electronics, Massachusetts Institute of Technology, Cambridge, MA 02139, USA

Abstract

Purpose—To compare optic disc perfusion between normal and glaucoma subjects using optical coherence tomography (OCT) angiography and detect optic disc perfusion changes in glaucoma.

Design—Observational, cross-sectional study.

Participants—Twenty-four normal subjects and 11 glaucoma patients were included.

Methods—One eye of each subject was scanned by a high-speed 1050 nm wavelength swept-source OCT instrument. The split-spectrum amplitude-decorrelation angiography algorithm (SSADA) was used to compute three-dimensional optic disc angiography. A disc flow index was computed from four registered scans. Confocal scanning laser ophthalmoscopy (cSLO) was used to measure disc rim area, and stereo photography was used to evaluate cup/disc ratios. Wide field OCT scans over the discs were used to measure retinal nerve fiber layer (NFL) thickness.

Main Outcome Measurements—Variability was assessed by coefficient of variation (CV). Diagnostic accuracy was assessed by sensitivity and specificity. Comparisons between glaucoma

Correspondence: David Huang, MD, PhD, davidhuang@alum.mit.edu, Weeks Professor of Ophthalmic Research, Casey Eye Institute, Oregon Health & Science University, 3375 S.W. Terwilliger Blvd. Portland, OR 97239-4197, USA, Phone (503) 4940633.

Disclosure

Publisher's Disclaimer: This is a PDF file of an unedited manuscript that has been accepted for publication. As a service to our customers we are providing this early version of the manuscript. The manuscript will undergo copyediting, typesetting, and review of the resulting proof before it is published in its final citable form. Please note that during the production process errors may be discovered which could affect the content, and all legal disclaimers that apply to the journal pertain.

and normal groups were analyzed by Wilcoxon rank-sum test. Correlations between disc flow index, structural assessments, and visual field (VF) parameters were assessed by linear regression.

Results—In normal discs, a dense microvascular network was visible on OCT angiography. This network was visibly attenuated in glaucoma subjects. The intra-visit repeatability, inter-visit reproducibility, and normal population variability of the optic disc flow index were 1.2%, 4.2%, and 5.0% CV respectively. The disc flow index was reduced by 25% in the glaucoma group (p = 0.003). Sensitivity and specificity were both 100% using an optimized cutoff. The flow index was highly correlated with VF pattern standard deviation ($R^2 = 0.752$, p = 0.001). These correlations were significant even after accounting for age, cup/disc area ratio, NFL, and rim area.

Conclusions—OCT angiography, generated by the new SSADA algorithm, repeatably measures optic disc perfusion. OCT angiography could be useful in the evaluation of glaucoma and glaucoma progression.

Glaucoma is the second leading cause of blindness in the United States.[1, 2] Although elevated intraocular pressure (IOP) is a risk factor, over half of glaucoma patients actually have IOPs within the normal range at their first visit.[3] There is a growing body of evidence suggesting that glaucoma pathogenesis is related to vascular dysfunction.[2, 4–6] More recently, prospective trials have demonstrated that optic disc hemorrhage [6–11] and peripapillary atrophy[12–14] are both associated with accelerated glaucoma progression. These findings may support a role for focal ischemia of the optic disc as a causative factor for glaucoma at least in some patients, either by itself or in conjunction with elevated IOP.

However, the lack of measurement tools has hampered the development of a clinical test for optic disc perfusion. Optical coherence tomography (OCT) is commonly used in clinical settings for the diagnosis and management of glaucoma.[15] Doppler OCT has been used to obtain precise measurements of total retinal blood flow calculated from the Doppler frequency shift of backscattered light.[15] While appropriate for large vessels around the disc, Doppler OCT is not sensitive enough to measure accurately the low velocities of small vessels that make up the disc microcirculation.

Recently, we developed a method of measuring local circulation using high-speed OCT to perform quantitative angiography. Using the split-spectrum amplitude-decorrelation angiography (SSADA) algorithm, flow in the optic disc can be quantified.[16] The purpose of this study was to investigate optic disc perfusion in glaucoma with OCT angiography, determine the relationship of flow index measurements with traditional measures of function and structure, and assess whether or not the SSADA-based optic disc flow index can measure vascular changes associated with glaucoma.

Methods

Study Population

This study was performed at the Casey Eye Institute at Oregon Health & Science University (OHSU). The research protocols were approved by the institutional review board at OHSU and carried out in accordance with the tenets of the Declaration of Helsinki. Written

informed consent was obtained from each subject following an explanation of the nature of the study.

The normal and early glaucoma subjects were part of the Advanced Imaging for Glaucoma (AIG) study. One eye from each subject was scanned and analyzed. Perimetric glaucoma (PG) eyes exhibited glaucomatous visual field (VF) loss and optic disc changes such as disc rim defects or nerve fiber layer defects on ophthalmoscopy. Preperimetric glaucoma (PPG) eyes showed similar changes to the optic disc as glaucomatous eyes while maintaining normal or borderline VF tests. Standard eye examinations and VF tests were performed on both eyes of the normal subjects. Normal VFs have a normal mean deviation (MD; P>0.05), pattern standard deviation (PSD; P>0.05), and glaucoma hemifield test (GHT; P>0.03). Glaucomatous VF loss was defined as either abnormal PSD (P<0.05) or GHT (P<1%) in a consistent pattern on both qualifying VF exams. Borderline VFs met neither normal nor PG criteria.

Optical Coherence Tomography

A swept-source based Fourier-domain OCT system described in previous publications[17, 18] was used to obtain images for the quantification of optic disc perfusion. The system utilized a commercially available swept laser centered at 1050 nm (Axsun Technologies, Inc., Billerica, MA, USA) with a 100 nm tuning range and operated at a 100 kHz repetition rate. This provided an axial resolution of 5.3 μm and an imaging range of 2.9 mm in tissue. Imaging of the optic disc was performed with an average laser output power of 1.9 mW, consistent with safety limits set by the American National Standards Institute (ANSI).[19]

Image Acquisition and Processing

Each subject underwent pupil dilation with 1% tropicamide and 2.5% phenylephrine eye drops prior to examination. Once dilated, subjects were seated in front of the OCT scanner, and their heads were stabilized with the aid of both a supporting chinrest and a forehead rest. Subjects were directed to focus their gaze on the internal fixation target, and a real-time *en face* view was used by the operator to visualize the imaging area on the fundus.

The scan pattern used was optimized for the SSADA algorithm.[18] Each set of scans was comprised of four 3 mm × 3 mm images of the optic disc obtained from 32,000 axial line scans. Two images in each set were captured in the x-fast configuration, with B-scans acquired rapidly along the x-axis. Each pass of the scan beam captured 200 axial lines forming a single B-scan. Eight B-scans were obtained at each fixed y-axis location before the process was repeated at the next sequential y-location. Two hundred sampling locations were covered along a 3-mm region of the y-axis. At a capture speed of 455 B-scans per second, the 1,600 B-scans were acquired within 3.5 seconds. The remaining two images in each set were captured in the y-fast configuration. While the data points remained the same between the y-fast and x-fast configuration, the order in which the data was collected differed. In the y-fast configuration, B-scans were acquired rapidly along the y-axis rather than the x-axis, as was performed in the x-fast configuration.

In each scan, the SSADA algorithm was used to distinguish vessels from static tissue. As seen in real-time OCT reflectance images, the amplitude of signal returning from nonstatic tissue varies rapidly over time.[18] By calculating the decorrelation of signal amplitude from consecutive B-scans, a contrast between static and nonstatic tissue is created that allows for the visualization of blood flow. The faster blood particles move across the laser beam, the higher is the decorrelation of the detected signals within a velocity range set by the scan parameters. Thus, decorrelation is approximately linear to flow velocity, i.e., the distance traveled by red blood cells flowing across the light beam per unit time.[20, 21] However, beyond a saturation velocity that is defined by the time interval between consecutive OCT B-scans, the decorrelation increases more slowly with velocity and eventually reaches an upper boundary.[21]

Eye motion causes two types of artifacts in SSADA. First, motion between consecutive B-scans at the same nominal position causes decorrelation that can appear as flow. Second, motion between B-scan positions distorts the transverse position of scans along the slow scan axis. To correct the first type of motion error, B-scans with very large (saccadic) bulk motion artifacts were removed. Furthermore, decorrelation due to bulk tissue motion was calculated by histogram analysis and subtracted from each cross-sectional SSADA frame.[18] To correct the second type of motion artifact, we used an image registration algorithm that registered 4 orthogonal raster scanned volumes.[22] Motion correction was first performed on the structural OCT data. The motion correction algorithm generated three-dimentional (3D) displacement fields that map A-scans from the input volumes into a common motion-corrected space. The same displacement fields were applied to the decorrelation (flow) data to produce motion-corrected flow data volumes. Flow data from four input volumes were weighted and merged,[22] improving the signal-to-noise ratio in the flow signal, and reducing the flow measurement variation due to local flow changes caused by the cardiac cycle.

Cross-sectional registered reflectance intensity images and flow images were summarized and viewed as an *en face* maximum projection. The disc boundary for each subject was manually delineated along the neural canal opening using the OCT reflectance images of normal (Fig. 1- A1, B1) and PG (Fig. 1 - A2, B2) eyes. The boundaries were then transferred to the OCT angiogram map (Fig. 1 - C1, C2) for disc region segmentation. The disc flow index was defined as the average decorrelation value within the disc, given by

$$\frac{\int_A D \cdot V dA}{\int_A dA} (\text{V}=1, \text{if vessel}; \text{V}=0, \text{if not})$$

where D was the decorrelation value acquired by SSADA. V was 1 when the decorrelation value was above background; otherwise, V was 0. Thus, the flow index is a dimensionless parameter between 0 and 1. Due to the nonlinear relationship between decorrelation and flow velocity, the flow index mainly measured the area (or caliber) of large vessels and both the area (or vessel density) and velocity of capillaries.

To clearly present the 3D nature of OCT angiography, the 3D angiogram was separately projected onto *en face* views (Fig. 1, panels E–G) in 3 layers. The segmentation was based

on the detection of the highest gradient magnitude in OCT reflectance for specific tissue interfaces (edges). The retinal layer was defined from the internal limiting membrane to the interpolated Bruch's membrane. The choroidal layer was defined as the layer 180 μm below the Bruch's membrane. The scleral layer was the region below the choroidal layer (Fig. 1 H1, H2).

Repeatability and Reproducibility

Intra-visit repeatability of the disc flow index was calculated from a subset of normal subjects with three sets of scans performed within a single visit. Each scan set, consisting of two x-fast and two y-fast scans, was obtained within 15 seconds of each other. The coefficient of variation (CV) was calculated by comparing three measurements obtained at the same location by a single operator.

The same subset of normal subjects used to calculate intra-visit repeatability were used to calculate inter-visit reproducibility obtained from three sets of scans performed on three separate visits. All scans were obtained within the timeframe of a year. The CV was determined from measurements made by a single operator and obtained on separate visits of the subjects.

Visual Field Testing

VF tests to determine pattern standard deviation (PSD) and mean deviation (MD) were performed with the Humphrey Field Analyzer II (Carl Zeiss Meditec, Inc., Dublin, CA, USA) set for the 24-2 threshold test, size III white stimulus and standard SITA algorithm.

Structural Analysis

The disc rim area for each subject was measured by confocal scanning laser ophthalmoscopy (cSLO) (HRT II, Heidelberg Engineering, GmbH, Dossenheim, Germany). An experienced glaucoma specialist graded vertical and horizontal cup-to-disc (C/D) ratio on stereo photography. The C/D area ratio was calculated by multiplying vertical and horizontal ratios. Additionally, peripapillary retinal nerve fiber layer (NFL) thickness was measured from a 3D volumetric scan of 8×8 mm on the same swept source OCT system used for OCT angiography. The NFL thickness was then averaged from a circular profile of 3.4 mm diameter centered on the disc.

Statistical Analysis

Linear regression analysis was employed in the normal group to investigate whether or not the measurement of disc flow index was affected by age, body mass index (BMI), mean ocular perfusion pressure (MOPP), or IOP. Wilcoxon rank-sum tests were used to compare average values of measurements between normal and glaucoma eyes. Univariate regression analysis was then used to determine the relationships between disc flow index and traditional measures of function and structure such as the VF MD, VF PSD, C/D area ratio, rim area, NFL thickness and IOP in the glaucoma group. Because VF values for MD and PSD were reported in logarithmic dB scale, values for disc flow index, C/D area ratio, rim area and NFL thickness were converted to logarithmic dB scale by 10×log10[value/(average value of the normal group)] to improve the correlation linearity and strengthen the

correlation coefficient values. Multivariate linear regression was performed after log transformation of the variable into dB units relative to the normal reference average. This model was used to analyze the effect of optic disc perfusion on the VF PSD test and vice versa while controlling for several other independent variables including age, C/D area ratio, rim area and NFL thickness. All statistical analyses were performed with Matlab version R2010b (MathWorks, Natick, MA, USA).

Results

Disc perfusion was studied in 24 normal and 11 glaucoma subjects (Table 1). The mean age in the normal group, 52 ± 10 years, was 16 years younger than the glaucoma group. The glaucoma group consisted of 8 PG and 3 PPG eyes. Most of the glaucoma group had mild disease in which 6 of the 11 subjects were stage 0 to 1 according to a Glaucoma Staging System 2.[23] There were no significant differences in BMI, diabetes mellitus, systemic hypertension, or the use of systemic antihypertensive medications between the two groups. There were also no significant differences between the control and glaucoma groups for IOP, diastolic blood pressure, systolic blood pressure, or MOPP. Data collection was complete except for cSLO and disc photography from one PPG subject.

The CV for intra-visit repeatability and inter-visit reproducibility of the disc flow index was 1.2% and 4.2%, respectively, based on measurements from 4 normal subjects. The inter-subject variability among the 24 normal subjects was 5.0% CV. There were no correlations of age, BMI, MOPP, or IOP with the disc flow index in the normal group. Three normal subjects (12%) were on systemic antihypertensive medications: 1 (4%) on a diuretic, and 2 (8%) on an angiotensin converting enzyme inhibitor. The use of any systemic antihypertensive medication or any subclass did not have a significant effect on disc flow index as determined by the Mann-Whitney U test.

There were no correlations of age, BMI, MOPP, or IOP with disc flow index in the glaucoma group. Four glaucoma subjects (36%) were on at least one systemic antihypertensive medication: 3 (27%) on a calcium channel blocker, 2 (18%) on a diuretic, 1 (9%) on an angiotensin receptor antagonist, and 1 (9%) on an angiotensin converting enzyme inhibitor. The use of any systemic antihypertensive medication or any subclass did not have a significant effect on the disc flow index as determined by the Mann-Whitney U test. Ten glaucoma subjects (91%) were on at least one ocular antihypertensive eye drop: 10 (91%) on a prostaglandin, 8 (73%) on a beta blocker, 4 (36%) on a carbonic anhydrase inhibitor, and 1 (9%) on an alpha-2 agonist. One (9%) used no drops, 2 (18%) used one drop, and 8 (73%) used more than one drop. Use of an ocular antihypertensive eye drop or any subclass was not correlated with the disc flow index as determined by the Mann-Whitney U test.

The OCT angiography scan provided detailed 3D image sets for both disc structure (reflectance) and perfusion (flow). Example images of normal and perimetric glaucoma eyes are shown in Figure 1. The color fundus photographs and OCT *en face* reflectance summation images both showed discs with moderate degrees of peripapillary atrophy. The maximum projection *en face* angiograms showed that normal discs had a denser

microvascular network (Fig. 1, C1, note dense microvascular network temporally) compared to the glaucomatous disc (Fig. 1, C2). The disc flow indices were computed by averaging decorrelation values within the disc margin in the *en face* whole depth OCT angiograms. The disc margin (ellipses in Fig. 1) could be determined from the *en face* structural OCT images, with the aid of color disc photographs. Cross-sectional OCT angiograms were constructed by overlaying blood flow (color scale) on reflectance (gray scale). These cross-sections showed that OCT angiography detected flow from all depths of the disc, from the inner surface to the lamina cribrosa. There appeared to be reduced flow in the lamina region of the glaucomatous disc compared to the normal disc (Fig. 1 - D1, D2).

The 3D OCT angiograms could also be projected within separate layers (Fig. 1, panels E–G). In examining these layered projections, one needs to keep in mind that large retinal vessels cast shadows on the tissue below. At the same time, flow from large superficial vessels can also be projected onto highly reflective tissue below, creating a flow projection artifact. This can occur because of variation in the shadowing effect due to the transit of blood particles. Thus large vessels in the retinal layer can be seen again in deeper layers as either shadows or flow. Despite these artifacts, distinct patterns were present in the layered *en face* projection angiograms. In the retinal layer, the superficial disc vasculature blended seamlessly into the retinal vascular network. The retinal and superficial disc vascular networks were dense in the normal eye (Fig. 1, E1), but attenuated in the glaucomatous eye (Fig. 1, E2). The peripapillary choroicapillaries were nearly confluent and dominated the choroidal layer angiograms (Fig. 1 F1, F2), but the disc circulation was relatively low in this layer. The sclera had relatively low flow and much of that was probably projected from the choroid above (Fig. 1 - G1, G2). The lamina cribrosa had a dense vascular network in the normal eye (Fig. 1, G1) and a mildly attenuated network in the glaucomatous eye (Fig. 1, G2). Based on all of the 3D information, the impression was that glaucoma attenuated flow in both the microvascular network of the superficial disc and in the deeper lamina cribrosa. The large retinal vessels appeared to be relatively unchanged in caliber.

The disc flow index in the glaucoma group was 25% lower (p = 0.003) compared to normal group (Fig. 2, Table 2). Sensitivity and specificity were both 100% using a flow index cutoff value of 0.1515 (Fig. 2). As expected, the glaucoma group also had significantly worse VF, rim area, C/D area ratio and NFL thickness (Table 2).

In the glaucoma group, univariate regression analysis showed that the disc flow index was significantly correlated with VF PSD and rim area, but not with VF MD, C/D area ratio, or NFL thickness (Table 3). The rim area was also significantly correlated with VF PSD, VF MD, C/D area ratio and NFL thickness. IOP was not significantly correlated with any other factors (data not shown).

In the normal group, there was no correlation between the disc flow index and age, VF PSD, rim area, C/D area ratio, or NFL thickness (Fig. 3). The glaucoma group tended to be older, had larger PSD and C/D ratio, smaller rim area and thinner NFL. In the glaucoma group the disc flow index was significantly correlated with VF PSD, and rim area (Fig. 3 and Table 3). It is notable that there was no overlap in flow index between the glaucoma and normal

groups, but there was much overlapping between the two groups for cSLO rim area, C/D area ratio and NFL thickness.

In the multivariate analysis where the flow index was considered as the dependent variable (Table 4), VF PSD was the dominant explanatory variable, accounting for ~75% of the variance (R^2). Age, C/D area ratio, rim area and NFL thickness were not significant explanatory variables when grouped with VF PSD in the multivariate models. This showed that disc perfusion was more strongly linked to VF PSD than any disc structural parameters. The PSD parameter was chosen to summarize VF function because it is a more specific diagnostic parameter than MD in early glaucoma.[24, 25]

In the multivariate analysis where the dependent variable was VF PSD (Table 5), the flow index was the dominant explanatory variable, accounting for ~75% of the variance (R^2). Age, C/D area ratio, and rim area were not significant explanatory variables when grouped with the disc flow index in the multivariate models. Although NFL thickness was a significant explanatory variable, the flow index was the dominant one, accounting for more than five times the variance (R^2) in VF PSD as NFL thickness. This suggests that the flow index is a relatively strong indicator of glaucoma severity.

Discussion

In this study, we reported the first use of OCT angiography to quantify human disc perfusion in glaucoma. OCT angiography with SSADA has many properties that make it useful for clinical evaluation. First, it is a noninvasive technique that does not require the injection of any exogenous dye or contrast agent. Second, it provides 3D visualization of the optic nerve head vasculature from the disc surface to the lamina cribrosa. Third, it provides near-automated quantification of disc perfusion for diagnostic evaluation.

Preliminary validation of the diagnostic utility of the disc flow index was shown by the significant differences between normal and glaucoma eyes. Further, there was a high correlation of the flow indices to visual functions, and low intra-visit, inter-visit, and inter-subject variability.

OCT angiography is not the first technique to be used to evaluate disc perfusion in glaucoma. Disc blood flow of glaucoma patients was previously investigated by fluorescein angiography (FA). Prolonged arteriovenous passage times have been demonstrated in patients with primary open-angle glaucoma[26] and normal pressure glaucoma.[27] Fluorescein filling defects in the disc have been found in glaucomatous[28] and ocular hypertensive eyes.[29] FA studies have also shown focal sector hypoperfusion of the optic disc in patients with low tension glaucoma and diffuse disc hypoperfusion in chronic simple glaucoma patients.[30] However, FA is not commonly used to monitor glaucoma due to its invasive nature and difficulty in quantification. Unlike FA, SSADA is a noninvasive technique that relies on the decorrelation of OCT signal amplitude reflected from nonstatic tissue. This allows for the quantification of flow that can be used to monitor disc perfusion while avoiding potential side effects of nausea and anaphylaxis associated with dye injection.[31, 32]

Laser Doppler flowmetry (LDF) and laser speckle flowgraphy (LSFG) are two other noninvasive techniques that were reported to measure disc perfusion. Using single-point LDF, Piltz-seymour et al. and Hamard et al. similarly reported decreased blood flow in the disc of glaucoma and glaucoma suspects when compared with normal subjects.[33, 34] Using scanning LDF, Michelson et al. reported that both neuroretinal rim blood flow and peripapillary retinal blood flow were significantly decreased in glaucoma patients compared with controls.[35] Hafez et al. also found significantly lower blood flow in the disc for open-angle glaucoma patients compared to normal patients and suggested perfusion might be reduced before the manifestation of visual field defects.[36] By use of LSFG, Yokoyama et al. found that the mean blur rate for the entire optic disc was significantly lower in the glaucoma group than that in the control group.[37] Sugiyama's group reported that less blood flow was observed with LSFG at the superior and inferior sectors of the disc rim in patients with PPG compared to normal control subjects.[38] Overall, our findings agree with previous results that disc perfusion is reduced in glaucomatous eyes. More importantly, OCT angiography with SSADA offers greater intra-visit repeatability (1.2% CV) and inter-visit reproducibility (4.2% CV) than either LSFG or LDF. With LSFG, CVs for intra-visit repeatability ranged from 1.9% – 11.9%, and inter-visit reproducibility was 12.8%.[39–43] LDF was even less reliable, with CVs for intra-visit repeatability of 6.6% – 21.2% and inter-visit reproducibility of 25.2% – 30.1%.[39, 44–47] Inter-subject variability in the normal population was also reduced when flow was assessed with SSADA-based OCT angiography (5.0%) compared with either LSFG (23.2% – 33%) or LDF (43.5% – 47.1%).[39, 41, 42, 45, 48]

A technical reason that SSADA has advantages over LDF is its relative insensitivity to variations in the average intensity of signal reflected from the tissue of interest, which could be affected by intrinsic tissue reflectance, or by beam attenuation due to defocus, media opacity, pigment absorption, and scattering in overlying tissue. In LDF, the variance of the speckle pattern is inherently proportional to average intensity of the reflected signal. In the SSADA algorithm, the effect of signal intensity is effectively cancelled because decorrelation is proportional to the variance divided by the average signal intensity.[18] This has been demonstrated clinically – the SSADA-based average decorrelation in three normal subjects varied within +/− 0.8% CV, even though the average signal intensity in the same images varied by +/− 36.7% CV.[16] Thus based on both theoretical considerations and clinical data, SSADA-based optic disc flow index is little affected by absorbance and reflectance of disc tissue, unlike LDF perfusion measurements. The reduced signal strength dependence by OCT angiography allows for cleaner inter-individual comparison of flow index.

With OCT angiography, the principal finding of the present study is the correlation between disc flow index and VF PSD ($R^2 = 0.752$, p = 0.001), which is suggestive of a link between reduced perfusion of the disc and severity of glaucoma. Multiple regression models (Tables 4 and 5) suggest that there is a strong link between VF PSD and disc flow index that is not mediated by disc structural variables such as C/D area ratio, rim area and NFL thickness. This suggests that the flow index provides independent information on glaucoma severity that is not available from structural variables alone. However, we also found in this study that the correlation between the disc flow index and VF MD was relatively low and not statistically significant. One explanation for the discrepancy between VF MD and PSD may

be that the MD is easily affected by nonglaucomatous factors, such as cataract, refractive error, and dry eye, and therefore less reliable in early glaucoma.[24, 25] Most of the glaucoma population in our study had early disease, therefore PSD may be a more reliable measure of their disease severity than MD. Another possibility for the better correlation of the flow index with PSD is that they both measure segmental or focal glaucomatous changes. In contrast, overall NFL thickness average and rim area are global measures that may correlate better with MD. Another explanation is that the discrepant correlations with MD and PSD are due to random variation because of the small sample size in our study. Thus our findings need confirmation from a larger independent study.

There are several limitations associated with OCT angiography. First, unlike Doppler OCT which provides absolute volumetric flow in μl/min, OCT angiography only yields a flow index in arbitrary units. However, the precision of the disc flow index measurement with OCT angiography is much better compared to dual-circular Doppler OCT scanning to measure the total retinal blood flow, which has an intra-visit repeatability of 10.5%.[49] Second, flow projection artifact from superficial blood vessels to deeper tissue levels prevents us from separately measuring superficial and deep ONH flow. The artifact is caused by the moving shadow cast by flowing blood cells. Decorrelation is caused by both moving reflectors, e.g., blood cells, and moving shadows, e.g., projections on distal high reflectance tissue. These two types of decorrelation are not distinguished by SSADA, and both appear as flow in the 3D angiogram. The artifact is not problematic if our analysis is confined to the 2D maximum projection angiogram. Therefore, the study was limited to the use of 2D angiograms that measured superficial and deep vascular beds together. Third, the disc flow index includes measurements on both the local disc circulation and the large retinal blood vessels. Thus it is a mixture of both disc and retinal circulations and not a pure measurement of a single vascular bed. However, due to the velocity saturation effect,[20, 21] OCT angiography, at current scan speeds, cannot measure flow, but it can measure the caliber of large vessels (see Fig. 1- E1, E2), suggesting angiography-based flow index mainly detects changes in disc microvasculature. The velocity or the blood flow in large retinal vessels should be measured using Doppler techniques.[50, 51] Fourth, OCT angiography requires the use of a high speed OCT system. In our study, we used a custom swept-source OCT device that operated at an axial scan rate of 100 kHz. Commercial spectral domain OCT devices typically operate at an axial scan rate of 20–40 kHz. However, recent advancements have led to the production of commercial spectral OCT devices operating at speeds of up to 70 kHz (RTVue XR, Optovue, Inc., Fremont, CA, USA; Cirrus HD-OCT 5000, Carl Zeiss Meditec, Dublin CA, USA), as well as a commercial 100 kHz swept-source OCT device (DRI OCT-1 Atlantis, Topcon Corp, Tokyo, Japan). Additionally, laboratory OCT prototypes of multi-MHz speed have already been reported.[52–54] Using these faster next-generation commercial OCT units, OCT angiography may become a feasible technique for clinical evaluation of glaucoma.

A notable limitation of our study is that we cannot rule out the effect of glaucoma and blood pressure medications on the disc flow index. Most patients in our glaucoma group were on multiple ocular antihypertensive eye drops. Therefore it is not possible to determine their individual effects on disc perfusion with our small sample size, and we cannot entirely rule out the possibility that the glaucoma drops could somehow be responsible for the reduced

disc perfusion. We consider this unlikely for two reasons. The first is the strong correlation between flow index and VF PSD that indicates perfusion is tightly linked to disease severity. The second is that previous studies have shown that select glaucoma eye drops, including prostaglandin,[55, 56] beta blockers,[57] and carbonic anhydrase inhibitors,[58, 59] either improved disc and retinal perfusion or had no significant effect.[60, 61] We plan to perform regional (i.e., superior and inferior hemisphere) correlation between VF and disc blood flow in a future study to remove entirely the confounding effect of global parameters such as medications from consideration.

In summary, we used OCT angiography based on the SSADA algorithm to measure human disc perfusion *in vivo*. We demonstrated that OCT angiography can detect reduced disc perfusion in a group of early glaucoma patients with 100% sensitivity and specificity. This reduction in flow index is not a byproduct of rim loss or cupping in glaucomatous eyes, and we were able to establish a strong link between the disc flow index and VF PSD.

We believe our data warrant further studies to determine if a lower flow index is correlated with the rate of progression and if disc perfusion can be used as a prognostic indicator for disease course. Potentially, flow index values may be used to help determine which ocular hypertensives and other glaucoma suspects require treatment. We anticipate that future investigations will lead to an enhanced understanding of this disease and improved treatment strategies.

Acknowledgments

References

1. Quigley HA, Broman AT. The number of people with glaucoma worldwide in 2010 and 2020. Br J Ophthalmol. 2006; 90:262–7. [PubMed: 16488940]

2. Leske MC. Open-angle glaucoma -- an epidemiologic overview. Ophthalmic Epidemiol. 2007; 14:166–72. [PubMed: 17896292]

3. Sommer A, Tielsch JM, Katz J, et al. Baltimore Eye Survey Research Group. Relationship between intraocular pressure and primary open angle glaucoma among white and black Americans. The Baltimore Eye Survey. Arch Ophthalmol. 1991; 109:1090–5. [PubMed: 1867550]

4. Flammer J. The vascular concept of glaucoma. Surv Ophthalmol. 1994; 38(suppl):S3–6. [PubMed: 7940146]

5. Bonomi L, Marchini G, Marraffa M, et al. Vascular risk factors for primary open angle glaucoma: the Egna-Neumarkt Study. Ophthalmology. 2000; 107:1287–93. [PubMed: 10889099]

6. Leske MC, Heijl A, Hyman L, et al. EMGT Group. Predictors of long-term progression in the Early Manifest Glaucoma Trial. Ophthalmology. 2007; 114:1965–72. [PubMed: 17628686]

7. Drance S, Anderson DR, Schulzer M. Collaborative Normal-Tension Glaucoma Study Group. Risk factors for progression of visual field abnormalities in normal-tension glaucoma. Am J Ophthalmol. 2001; 131:699–708. [PubMed: 11384564]

8. Bengtsson B, Leske MC, Yang Z, Heijl A. EMGT Group. Disc hemorrhages and treatment in the Early Manifest Glaucoma Trial. Ophthalmology. 2008; 115:2044–8. [PubMed: 18692244]

9. De Moraes CG, Juthani VJ, Liebmann JM, et al. Risk factors for visual field progression in treated glaucoma. Arch Ophthalmol. 2011; 129:562–8. [PubMed: 21555607]

10. Leske MC, Heijl A, Hussein M, et al. Early Manifest Glaucoma Trial Group. Factors for glaucoma progression and the effect of treatment: the Early Manifest Glaucoma Trial. Arch Ophthalmol. 2003; 121:48–56. [PubMed: 12523884]

11. Suh MH, Park KH, Kim H, et al. Glaucoma progression after the first-detected optic disc hemorrhage by optical coherence tomography. J Glaucoma. 2012; 21:358–66. [PubMed: 21623225]

12. See JL, Nicolela MT, Chauhan BC. Rates of neuroretinal rim and peripapillary atrophy area change: a comparative study of glaucoma patients and normal controls. Ophthalmology. 2009; 116:840–7. [PubMed: 19410941]

13. Uchida H, Ugurlu S, Caprioli J. Increasing peripapillary atrophy is associated with progressive glaucoma. Ophthalmology. 1998; 105:1541–5. [PubMed: 9709771]

14. Jonas JB, Grundler AE. Correlation between mean visual field loss and morphometric optic disk variables in the open-angle glaucomas. Am J Ophthalmol. 1997; 124:488–97. [PubMed: 9323939]

15. Wang Y, Bower BA, Izatt JA, et al. Retinal blood flow measurement by circumpapillary Fourier domain Doppler optical coherence tomography. J Biomed Opt. 2008; 13:064003. [PubMed: 19123650]

16. Jia Y, Morrison JC, Tokayer J, et al. Quantitative OCT angiography of optic nerve head blood flow. Biomed Opt Express [serial online]. 2012; 3:3127–37. Available at: http://www.opticsinfobase.org/boe/fulltext.cfm?uri=boe-3-12-3127&id=245369.

17. Potsaid B, Baumann B, Huang D, et al. Ultrahigh speed 1050nm swept source/Fourier domain OCT retinal and anterior segment imaging at 100,000 to 400,000 axial scans per second. Opt Express [serial online]. 2010; 18:20029–48. Available at: http://www.opticsinfobase.org/oe/abstract.cfm?uri=oe-18-19-20029.

18. Jia Y, Tan O, Tokayer J, et al. Split-spectrum amplitude-decorrelation angiography with optical coherence tomography. Opt Express [serial online]. 2012; 20:4710–25. Available at: http://www.opticsinfobase.org/oe/fulltext.cfm?uri=oe-20-4-4710&id=227624.

19. American National Standard for Safe Use of Lasers, ANSI Z136.1–2007. Orlando, FL: Laser Institute of America; 2007.

20. Tokayer J, Jia Y, Dhalla AH, Huang D. Blood flow velocity quantification using split-spectrum amplitude-decorrelation angiography with optical coherence tomography. Biomed Opt Express [serial online]. 2013; 4:1909–24. Available at: http://www.opticsinfobase.org/boe/fulltext.cfm?uri=boe-4-10-1909&id=260835.

21. Liu G, Lin AJ, Tromberg BJ, Chen Z. A comparison of Doppler optical coherence tomography methods. Biomed Opt Express [serial online]. 2012; 3:2669–80. Available at: http://www.opticsinfobase.org/boe/fulltext.cfm?uri=boe-3-10-2669&id=242508.

22. Kraus MF, Potsaid B, Mayer MA, et al. Motion correction in optical coherence tomography volumes on a per A-scan basis using orthogonal scan patterns. Biomed Opt Express [serial online]. 2012; 3:1182–99. Available at: http://www.opticsinfobase.org/boe/fulltext.cfm?uri=boe-3-6-1182&id=233031.

23. Brusini P, Filacorda S. Enhanced Glaucoma Staging System (GSS 2) for classifying functional damage in glaucoma. J Glaucoma. 2006; 15:40–6. [PubMed: 16378017]

24. Bengtsson B, Heijl A. A visual field index for calculation of glaucoma rate of progression. Am J Ophthalmol. 2008; 145:343–53. [PubMed: 18078852]

25. Gordon MO, Beiser JA, Brandt JD, et al. Ocular Hypertension Treatment Study Group. The Ocular Hypertension Treatment Study: baseline factors that predict the onset of primary open-angle glaucoma. Arch Ophthalmol. 2002; 120:714–20. [PubMed: 12049575]

26. Arend O, Plange N, Sponsel WE, Remky A. Pathogenetic aspects of the glaucomatous optic neuropathy: fluorescein angiographic findings in patients with primary open angle glaucoma. Brain Res Bull. 2004; 62:517–24. [PubMed: 15036566]

27. Huber K, Plange N, Remky A, Arend O. Comparison of colour Doppler imaging and retinal scanning laser fluorescein angiography in healthy volunteers and normal pressure glaucoma patients. Acta Ophthalmol Scand. 2004; 82:426–31. [PubMed: 15291936]

28. Talusan E, Schwartz B. Specificity of fluorescein angiographic defects of the optic disc in glaucoma. Arch Ophthalmol. 1977; 95:2166–75. [PubMed: 588109]

29. Schwartz B, Rieser JC, Fishbein SL. Fluorescein angiographic defects of the optic disc in glaucoma. Arch Ophthalmol. 1977; 95:1961–74. [PubMed: 921573]

30. Hitchings RA, Spaeth GL. Fluorescein angiography in chronic simple and low-tension glaucoma. Br J Ophthalmol. 1977; 61:126–32. [PubMed: 843509]

31. Hayreh SS, Hayreh MS. Optic disc edema in raised intracranial pressure. II. Early detection with fluorescein fundus angiography and stereoscopic color photography. Arch Ophthalmol. 1977; 95:1245–54. [PubMed: 406883]

32. Stein MR, Parker CW. Reactions following intravenous fluorescein. Am J Ophthalmol. 1971; 72:861–8. [PubMed: 5119698]

33. Piltz-Seymour JR, Grunwald JE, Hariprasad SM, Dupont J. Optic nerve blood flow is diminished in eyes of primary open-angle glaucoma suspects. Am J Ophthalmol. 2001; 132:63–9. [PubMed: 11438055]

34. Hamard P, Hamard H, Dufaux J, Quesnot S. Optic nerve head blood flow using a laser Doppler velocimeter and haemorheology in primary open angle glaucoma and normal pressure glaucoma. Br J Ophthalmol. 1994; 78:449–53. [PubMed: 8060927]

35. Michelson G, Langhans MJ, Groh MJ. Perfusion of the juxtapapillary retina and the neuroretinal rim area in primary open angle glaucoma. J Glaucoma. 1996; 5:91–8. [PubMed: 8795740]

36. Hafez AS, Bizzarro RL, Lesk MR. Evaluation of optic nerve head and peripapillary retinal blood flow in glaucoma patients, ocular hypertensives, and normal subjects. Am J Ophthalmol. 2003; 136:1022–31. [PubMed: 14644212]

37. Yokoyama Y, Aizawa N, Chiba N, et al. Significant correlations between optic nerve head microcirculation and visual field defects and nerve fiber layer loss in glaucoma patients with myopic glaucomatous disk. Clin Ophthalmol. 2011; 5:1721–7. [PubMed: 22205831]

38. Sugiyama, T.; Shibata, M.; Kojima, S.; Ikeda, T. Optic nerve head blood flow in glaucoma. In: Kubena, T., editor. The Mystery of Glaucoma [book online]. Rijeka, Croatia: InTech; 2011. Available at: http://www.intechopen.com/books/the-mystery-of-glaucoma/optic-nerve-head-blood-flow-in-glaucoma [Accessed December 24, 2013]

39. Yaoeda K, Shirakashi M, Funaki S, et al. Measurement of microcirculation in the optic nerve head by laser speckle flowgraphy and scanning laser Doppler flowmetry. Am J Ophthalmol. 2000; 129:734–9. [PubMed: 10926981]

40. Aizawa N, Yokoyama Y, Chiba N, et al. Reproducibility of retinal circulation measurements obtained using laser speckle flowgraphy-NAVI in patients with glaucoma. Clin Ophthalmol. 2011; 5:1171–6. [PubMed: 21887100]

41. Yaoeda K, Shirakashi M, Fukushima A, et al. Relationship between optic nerve head microcirculation and visual field loss in glaucoma. Acta Ophthalmol Scand. 2003; 81:253–9. [PubMed: 12780404]

42. Yaoeda K, Shirakashi M, Funaki S, et al. Measurement of microcirculation in optic nerve head by laser speckle flowgraphy in normal volunteers. Am J Ophthalmol. 2000; 130:606–10. [PubMed: 11078839]

43. Tamaki Y, Araie M, Tomita K, et al. Real-time measurement of human optic nerve head and choroid circulation, using the laser speckle phenomenon. Jpn J Ophthalmol. 1997; 41:49–54. [PubMed: 9147189]

44. Kagemann L, Harris A, Chung HS, et al. Heidelberg retinal flowmetry: factors affecting blood flow measurement. Br J Ophthalmol. 1998; 82:131–6. [PubMed: 9613377]

45. Luksch A, Lasta M, Polak K, et al. Twelve-hour reproducibility of retinal and optic nerve blood flow parameters in healthy individuals. Acta Ophthalmol. 2009; 87:875–80. [PubMed: 18976308]

46. Nicolela MT, Hnik P, Schulzer M, Drance SM. Reproducibility of retinal and optic nerve head blood flow measurements with scanning laser Doppler flowmetry. J Glaucoma. 1997; 6:157–64. [PubMed: 9211138]

47. Iester M, Altieri M, Michelson G, et al. Intraobserver reproducibility of a two-dimensional mapping of the optic nerve head perfusion. J Glaucoma. 2002; 11:488–92. [PubMed: 12483092]

48. Jonescu-Cuypers CP, Harris A, Bartz-Schmidt KU, et al. Reproducibility of circadian retinal and optic nerve head blood flow measurements by Heidelberg retina flowmetry. Br J Ophthalmol. 2004; 88:348–53. [PubMed: 14977767]

49. Wang Y, Lu A, Gil-Flamer J, et al. Measurement of total blood flow in the normal human retina using Doppler Fourier-domain optical coherence tomography. Br J Ophthalmol. 2009; 93:634–7. [PubMed: 19168468]

50. Wang Y, Bower BA, Izatt JA, et al. Retinal blood flow measurement by circumpapillary Fourier domain Doppler optical coherence tomography. J Biomed Opt. 2008; 13:064003. [PubMed: 19123650]

51. Wang Y, Fawzi AA, Varma R, et al. Pilot study of optical coherence tomography measurement of retinal blood flow in retinal and optic nerve diseases. Invest Ophthalmol Vis Sci. 2011; 52:840–5. [PubMed: 21051715]

52. Choi DH, Hiro-Oka H, Shimizu K, Ohbayashi K. Spectral domain optical coherence tomography of multi-MHz A-scan rates at 1310 nm range and real-time 4D-display up to 41 volumes/second. Biomed Opt Express [serial online]. 2012; 3:3067–86. Available at: http://www.opticsinfobase.org/boe/fulltext.cfm?uri=boe-3-12-3067&id=244867.

53. Klein, T.; Wieser, W.; André, R., et al. Multi-MHz FDML OCT: snapshot retinal imaging at 6.7 million axial-scans per second. In: Izatt, JA.; Fukimoto, JG.; Tuchin, VV., editors. Optical Coherence Tomography and Coherence Domain Optical Methods in Biomedicine XVI; Proceedings of SPIE--the International Society for Optical Engineering; San Francisco, CA: SPIE; 2012. p. 82131E

54. Potsaid, B.; Jayaraman, V.; Fujimoto, JG., et al. MEMS tunable VCSEL light source for ultrahigh speed 60kHz - 1MHz axial scan rate and long range centimeter class OCT imaging. In: Izatt, JA.; Fukimoto, JG.; Tuchin, VV., editors. Optical Coherence Tomography and Coherence Domain Optical Methods in Biomedicine XVI; Proceedings of SPIE--the International Society for Optical Engineering; San Francisco, CA: SPIE; 2012. p. 82130M

55. Tamaki Y, Nagahara M, Araie M, et al. Topical latanoprost and optic nerve head and retinal circulation in humans. J Ocul Pharmacol Ther. 2001; 17:403–11. [PubMed: 11765145]

56. Makimoto Y, Sugiyama T, Kojima S, Azuma I. Long-term effect of topically applied isopropyl unoprostone on microcirculation in the human ocular fundus. Jpn J Ophthalmol. 2002; 46:31–5. [PubMed: 11853711]

57. Tamaki Y, Araie M, Tomita K, Nagahara M. Effect of topical betaxolol on tissue circulation in the human optic nerve head. J Ocul Pharmacol Ther. 1999; 15:313–21. [PubMed: 10463870]

58. Tamaki Y, Araie M, Muta K. Effect of topical dorzolamide on tissue circulation in the rabbit optic nerve head. Jpn J Ophthalmol. 1999; 43:386–91. [PubMed: 10580660]

59. Ohguro I, Ohguro H. The effects of a fixed combination of 0. 5% timolol and 1% dorzolamide on optic nerve head blood circulation. J Ocul Pharmacol Ther. 2012; 28:392–6. [PubMed: 22480163]

60. Costa VP, Harris A, Stefánsson E, et al. The effects of antiglaucoma and systemic medications on ocular blood flow. Prog Retin Eye Res. 2003; 22:769–805. [PubMed: 14575724]

61. Mayama C, Araie M. Effects of antiglaucoma drugs on blood flow of optic nerve heads and related structures. Jpn J Ophthalmol. 2013; 57:133–49. [PubMed: 23321913]
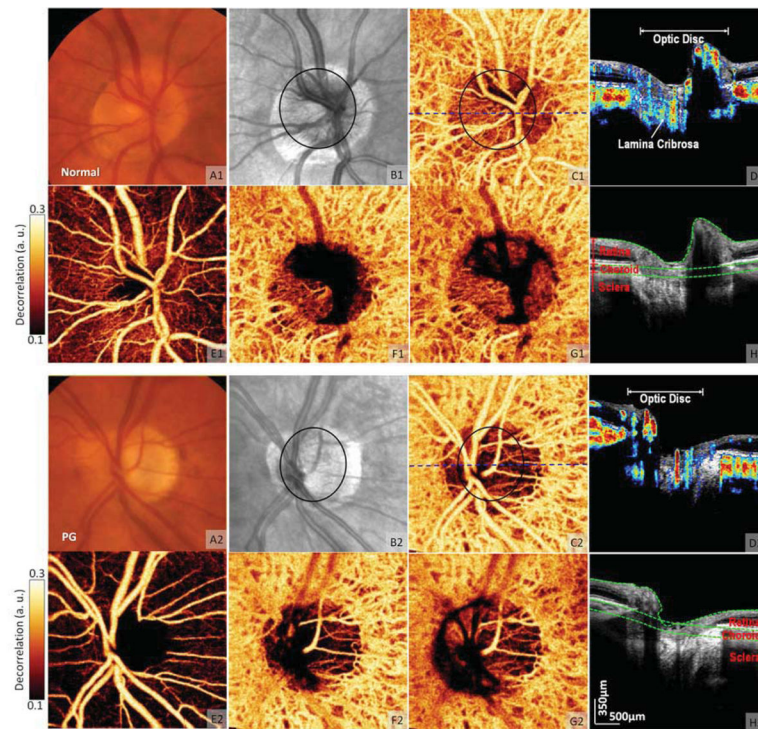
Figure 1.
Disc photographs (A1, A2), optical coherence tomography (OCT) reflectance (B1, B2), whole depth OCT angiograms (C1, C2, *en face* maximum projection), cross-sectional angiograms (D1, D2, overlaying on OCT reflectance in gray scale) in the right eye of a normal subject (A1-H1) and, the left eye of a perimetric glaucoma subject (A2-H2). Disc margins are marked by the black elliptical outlines (B1, B2, C1, C2). The position of the cross-section is shown by dotted blue lines (C1, C2). A dense microvascular network was visible on the OCT angiography of the normal disc (C1). This network was greatly attenuated in the glaucomatous disc (C2). In order to appreciate the ability of OCT angiography to detect blood flow within the various vascular beds, the 3D angiograms were separately projected into *en face* maximum projection in 3 layers, i.e. retinal angiograms (E1, E2), choroidal angiograms (F1, F2) and scleral/lamina cribrosa angiograms (G1, G2). The boundaries used for segmentation are indicated by dotted green lines on cross-sectional OCT reflectance (H1, H2).

Figure 2.
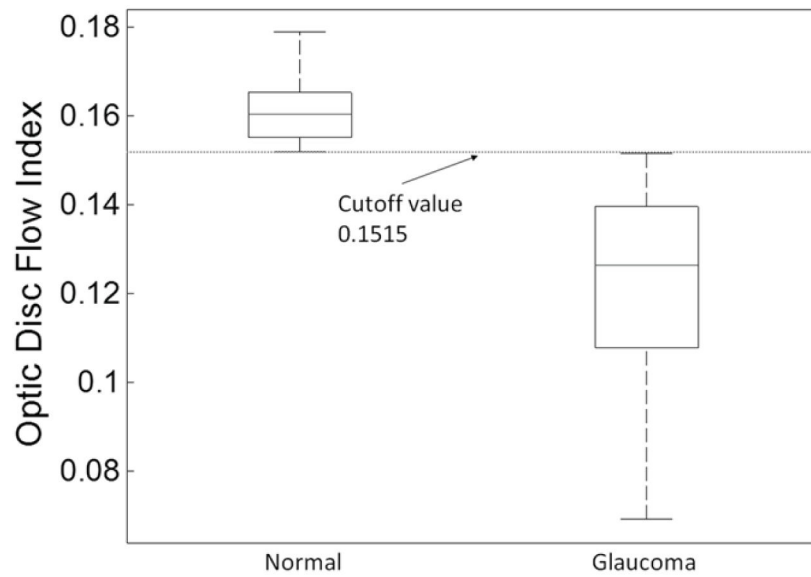Box plot showing the disc flow index in normal and glaucoma groups. The median (line inside the box), interquartile range (box) and the whole range of values (whiskers) are shown. This plot shows that the two groups are completely separated. The minimum of normal group is 0.1516, and the maximum of glaucoma group is 0.1513, indicating sensitivity and specificity are both 100% using a cutoff value of 0.1515.
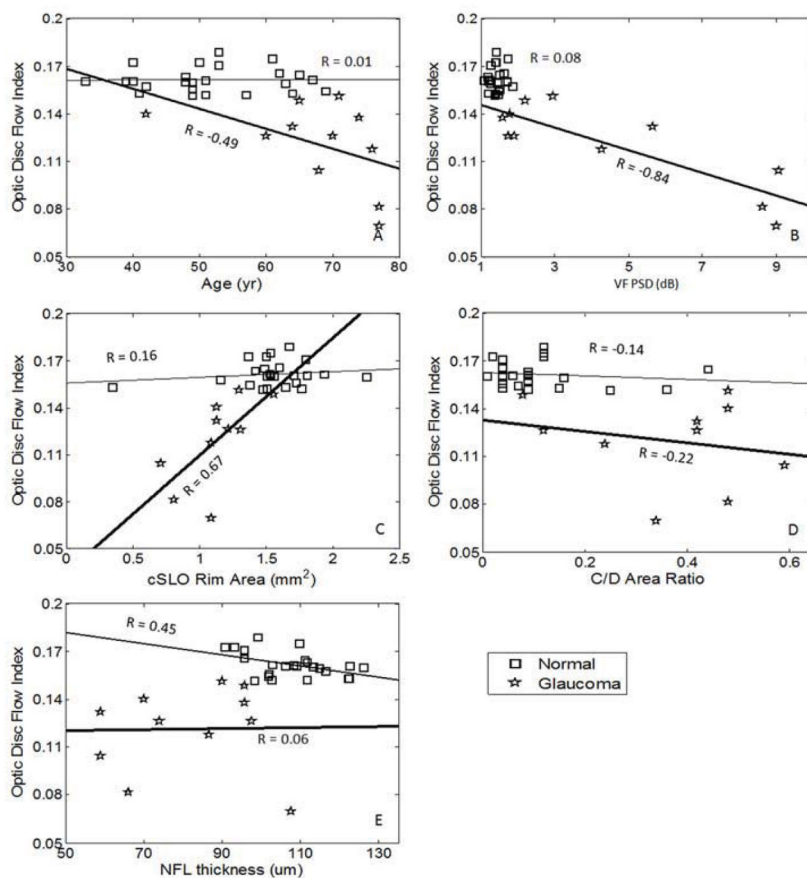
Figure 3.
Plots of disc flow index versus age (A), pattern standard deviation (PSD) (B), rim area (C), cup/disc (C/D) area ratio (D) and nerve fiber layer (NFL) thickness (E) in both normal group and glaucoma group. The linear regression trend lines are gray in the normal group and black in the glaucoma group.

Table 1

Characteristics of Normal and Glaucoma Subjects

Characteristic		Normal	Glaucoma	P-value[†]
Patients, n		24	11	
Eyes, n		24	11	
Age (Years)		52 ± 10	68 ± 10	0.000
Body Mass Index(BMI)		29.2 ± 6.0	28.6 ± 6.7	0.800
Diabetes Mellitus, n (%)		1 (4%)	0 (0%)	1.00*
Systemic Hypertension, n (%)		3 (13%)	4 (36%)	0.171*
Taking Systemic Antihypertensive Medication, n (%)		3 (13%)	4 (36%)	0.171*
Taking Ocular Antihypertensive Eye drops, n (%)		0 (0%)	10 (91%)	0.001*
Intraocular Pressure (mm Hg)		15.27 ± 2.3	13.59 ± 3.9	0.118
Diastolic Blood Pressure (mm Hg)		80.6 ± 6.9	78.1 ± 11.5	0.510
Systolic Blood Pressure (mm Hg)		124.4 ± 12.8	125.7 ± 9.5	0.764
Mean Ocular Perfusion Pressure (mm Hg)		48.21 ± 5.1	49.05 ± 5.7	0.662
	Stage 0	24	2	
	Stage b	0	3	
Glaucoma Staging Subgroups[#]	Stage 1	0	1	
	Stage 2	0	1	
	Stage 3	0	3	
	Stage 4	0	1	

[†] All calculated by t-test, except the values marked by * which were calculated by chi-square test.

[#] Glaucoma cases were classified by the enhanced Glaucoma Staging System (GSS 2).[23]

Table 2

Results of Diagnostic Testing

	Variables	Normal	Glaucoma	P-Value[†]
Visual Field	MD (dB)	0.20 ± 0.87 (−1.59~1.87)	−3.28 ± 4.12 (−13.35~0.08)	0.003
	PSD (dB)	1.43 ± 0.20 (1.10~1.86)	4.44 ± 3.12 (1.59~9.07)	0.003
Structural Assessments	cSLO Rim Area (mm²)	1.55 ± 0.34 (0.35~2.26)	1.13 ± 0.25 (0.71~1.56)	0.007
	Cup/Disc Area Ratio	0.11 ± 0.10 (0.01~0.44)	0.37 ± 0.17 (0.08~0.59)	0.012
	NFL Thickness (μm)	107.9±9.9 (90.8~122.6)	82.0±17.0 (58.9~107.6)	0.000
Disc Perfusion	Flow Index	0.161 ± 0.008 (0.15~0.18)	0.121 ± 0.0263(0.07~0.15)	0.003

Numbers displayed are mean ± population standard deviation (range); MD = mean deviation, PSD = pattern standard deviation; cSLO = confocal scanning laser ophthalmoscopy; NFL= nerve fiber layer.

[†]Wilcoxon rank sum

Table 3

Correlation Coefficient Matrix among Visual Field, Blood Flow, and Structural Variables in Glaucoma Subjects

Variables (dB)	Disc Flow Index	Visual Field MD	Visual Field PSD	C/D Area Ratio	cSLO Rim Area
VF MD	0.138 (0.146) [†]				
VF PSD	**0.752 (0.001)**	**0.563 (0.006)**			
C/D Area Ratio	0.048 (0.273)	**0.307 (0.048)**	0.201 (0.097)		
cSLO Rim Area	**0.397 (0.026)**	**0.724 (0.001)**	**0.638 (0.003)**	**0.371 (0.031)**	
NFL Thickness	0.004 (0.853)	**0.508 (0.014)**	0.121 (0.294)	0.138 (0.289)	**0.408 (0.047)**

All variables were converted to dB scale by 10×log10 [value/(average value of the normal group)]. Table cells display Pearson's R^2 (P-value to test |R| =0). Statistically significant correlations (P < 0.05) are bold faced. VF = visual field, MD = mean deviation, PSD = pattern standard deviation, C/D = cup/disc, cSLO = confocal scanning laser ophthalmoscopy, IOP = intraocular pressure, NFL= nerve fiber layer.

Table 4

Multivariate Regression Models of Factors Affecting Disc Flow Index in Glaucoma Subjects

Model	Variable 1			Variable 2			
	Variable (dB)	Slope (P-value)	R^2	Variable (dB)	Slope (P-value)	R^2	Total R^2
1	PSD	**−0.319 (0.001)**	0.75				
2	PSD	**−0.312 (0.002)**	0.75	Age	−0.067 (0.828)	0.001	0.751
3	PSD	**−0.367 (0.002)**	0.752	C/D Area Ratio	0.088 (0.306)	0.037	0.789
4	PSD	**−0.383 (0.013)**	0.752	cSLO Rim Area	0.207 (0.585)	0.012	0.764
5	PSD	**−0.332 (0.000)**	0.702	NFL Thickness	−0.388 (0.086)	0.097	0.799

All variables were converted to dB scale by 10×log10 [value/(average value of the normal group)]. Significant slope coefficients (P < 0.05) are bold faced. PSD = pattern standard deviation, C/D = cup/disc, cSLO = confocal scanning laser ophthalmoscopy, NFL = nerve fiber layer.

Table 5

Multivariate Regression Models of Factors Affecting Visual Field Pattern Standard Deviation in Glaucoma Subjects

	Variable 1			Variable 2			
Model	Variable (dB)	Slope (P-value)	R^2	Variable (dB)	Slope (P-value)	R^2	Total R^2
1	Disc Flow Index	−2.353 (**0.001**)	0.75				
2	Disc Flow Index	−2.254(**0.002**)	0.75	Age	0.373 (0.649)	0.006	0.756
3	Disc Flow Index	−2.123 (**0.002**)	0.752	C/D Area Ratio	0.295 (0.138)	0.071	0.823
4	Disc Flow Index	−1.587 (**0.013**)	0.752	cSLO Rim Area	−1.303 (0.056)	0.106	0.858
5	Disc Flow Index	−2.405 (**0.000**)	0.702	NFL Thickness	−1.167 (**0.047**)	0.121	0.823

All variables were converted to dB scale by 10×log10 [value/(average value of the normal group)]. Significant slope coefficients (P < 0.05) are bold faced. C/D = cup/disc, cSLO = confocal scanning laser ophthalmoscopy, NFL = nerve fiber layer.